

# Chapter 1

## Estimating the In-Plane Lateral Resistance of Reinforced Log Wall Employing Soft Modelling Techniques

**K. G. M. Kandethanthri**

*Concordia University, Canada*

**Mehdi Nikoo**

*Concordia University, Canada*

**Ghazanfarah Hafeez**

 <https://orcid.org/0000-0002-5045-6968>

*Concordia University, Canada*

**Ashutosh Bagchi**

*Concordia University, Canada*

**Vagelis Plevris**

 <https://orcid.org/0000-0002-7377-781X>

*Qatar University, Qatar*

### ABSTRACT

*The popularity of log houses has been on the rise in numerous regions worldwide. In the context of log construction, the stability of log walls is notably influenced by the friction existing between the layers of logs and the openings designated for windows and doors. This study endeavors to comprehensively evaluate the lateral resistance of log walls through an extensive parametric analysis utilizing finite element (FE) methods. To construct a robust dataset, a total of 71 distinct samples were generated employing FE analysis, where the shuffled frog-leaping algorithm (SFLA) was incorporated in conjunction with a feed-forward (FF) neural network. Within this framework, the accuracy of the SFLA-based informational model was juxtaposed against that of an artificial neural network (ANN) coupled with particle swarm optimization (PSO), genetic algorithm (GA), and statistical models including multiple linear regression (MLR).*

DOI: 10.4018/979-8-3693-2161-4.ch001

## INTRODUCTION

Log houses were introduced to Canada through European newsletters. The renewed interest in wood as a construction material, driven by concerns about climate change, has led to increased attention towards this construction technology in various regions around the world. Contemporary log construction incorporates larger windows and door openings, featuring a diverse range of layouts and aspect ratios. The structural integrity of a log house relies on several factors, including wall dimensions, the arrangement of openings, and the methods employed to support the logs around these openings, as openings are known to lessen the structural strength of log walls (Bedon, Rinaldin, et al., 2015). Schematics of typical log walls with and without window and door openings are provided in Figure 1.

During the last three decades, several researchers have focused on investigating the lateral performance of log walls under various loading conditions employing experimental (Branco & Araújo, 2010; De Araujo et al., 2016; Eakintumas et al., 2022; Sciomenta et al., 2018), and numerical modeling methods (Kalantari et al., 2021; Kalantari & Hafeez, 2021; Kandethanthri & Hafeez, 2023; Rinaldin et al., 2013). The authors also explored the resistance of such a wall system under lateral (Bedon, Rinaldin, et al., 2015; Bedon & Fragiaco, 2017; Heimeshoff & Kneidl, 1990, 1992) and fire loads (Bedon & Fragiaco, 2019). Further, Scott et al., 2005, reported on the effects of foundation anchorage systems on the wall system's structural behavior (Scott et al., 2005).

Timber is characterized as an anisotropic material, exhibiting greater strength along the axis parallel to its fiber direction, whereas its capacity to withstand loads orthogonal to the fiber direction is comparatively diminished. The load transfer phenomenon in the log wall is different than the conventional wood frame wall. Unlike a conventional wood shear wall, the transmission of load to the foundation transpires via compressive stress perpendicular to the grain. The wall's vertical stability is ensured through strategically placed notches and diverse corner styles. Horizontal load-bearing resistance is facilitated by the frictional force and the interlocking mechanism inherent to the logs' arrangement (Hahney, 2000).

The structural integrity of log walls, in the context of resisting lateral forces, is primarily achieved through mechanisms that are ingeniously integrated into their construction. It has been recognized that the friction generated by the weight of the logs pressing against one another plays a crucial role in this context (Branco & Araújo, 2012). This natural resistance is significantly enhanced by the architectural design of interlocking corners, where logs are precisely notched and joined together, allowing for the effective distribution of lateral loads across the structure. Furthermore, the addition of mechanical fasteners such as screws, bolts, and wooden dowels has been identified as a modern technique to secure the logs more tightly, thereby providing an additional layer of stability against lateral pressures (Graham Drew, A. et al., 2010). This amalgamation of traditional craftsmanship and contemporary engineering not only augments the aesthetic allure of log structures but also substantially elevates their capacity to withstand environmental forces. Hence, the deliberate application of these construction principles signifies a pivotal enhancement in the field of log wall construction, ensuring their enduring resilience and safety.

Lateral performance of the log wall was assessed experimentally on the wall with logs of swedish cope profile in various configurations, including steel and wood pins. The authors reported the lowest lateral load resistance of the walls without corner style and pins (Popovski et al., 2002). Later the in-plane performance of log walls with rectangular log profiles and various transversal stiffnesses was assessed, and the study determined an increase in lateral stiffness with an increased pre-compression load (Branco & Araújo, 2012). The walls with rectangular profiles and various corner styles were tested under monotonic and cyclic loads. The authors reported higher lateral resistance and energy dissipation

of the wall with standard joints (Bedon, Massimo, et al., 2015). Furthermore, an exploration into the seismic response of full-scale log shear walls was conducted through the utilization of finite element methods. This inquiry resulted in the determination of a linear correlation between energy dissipation and axial load, as well as an inverse correlation between the height of the log wall and post-elastic stiffness (Grossi et al., 2016).

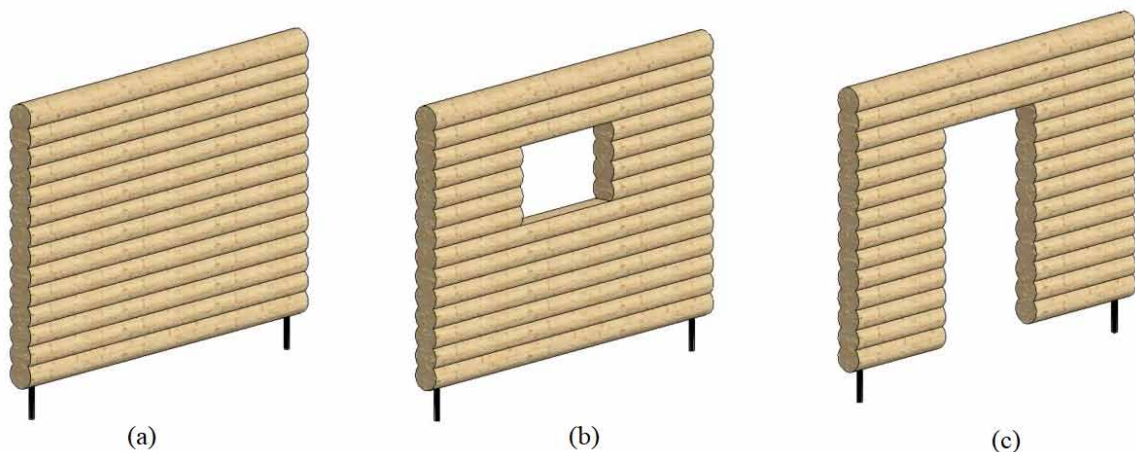
Artificial neural networks (ANNs) have proven to be highly effective in modeling timber materials and structures (Nikoo et al., 2023). Previous research has used ANNs for a variety of tasks, such as estimating the mechanical properties of wood (Ma et al., 2022), evaluating compression strength in heat-treated woods (Tiryaki & Aydın, 2014), and analyzing wood bonding quality (Bardak et al., 2016). This study combines ANNs with Finite Element Modeling (FEM) to estimate output parameters and fill the knowledge gap in the lateral performance of log walls. The present study leveraged the combination of ANNs and optimization algorithms to assess the predictability of the maximum resistance force in log walls. The subsequent section provides an overview of ANNs, followed by a concise examination of the optimization algorithms that were implemented.

## **BACKGROUND**

### **Artificial Neural Network**

An ANN is a computational system adept at learning from past experiences and extrapolating that knowledge to novel datasets (Adeli, 2001; Ian & Nabil, 1994). These networks acquire knowledge by executing systematic computations that emulate the inherent processes within a dataset, resembling the cognitive mechanisms of the human brain. In this investigation, multilayer feed-forward networks were employed to predict the in-plane lateral resistance of reinforced log walls. This configuration encompasses distinct layers, including input, hidden, and output layers, which collectively facilitate the forward propagation of the ANN. Each layer, comprised of neuronal nodes (neurons), establishes con-

*Figure 1. Log wall with Swedish cope log profiles (a) wall without opening, (b) wall with window opening, (c) wall with door opening*



nections with the preceding layer, thereby enabling the intricate information flow within the network. Neurons in the hidden and output layers are composed of weights, biases, and activation functions that can be continuous, linear, or nonlinear. The standard activation functions (Nikoo et al., 2018) consisting of nonlinear sigmoid functions (logsig, tansig) and linear functions (poslin, purelin) help determine and transfer the weight and bias in the subsequent layers. Once the structure of feed-forward model is recognized, the weights and biases are modified by employing training techniques. This study uses the Levenberg Marquardt (LM) methodology as a training technique (Bishop, 2006; Haykin, 2008), followed by implementing the optimization algorithm for weight and bias to reduce the errors. Finally, the LM methodology, which distributes network errors to achieve an optimal fit or minimize errors, is employed as a reliable ANN training method.

## **Optimization Algorithms**

### **Shuffled Frog Leaping Algorithm (SFLA)**

The SFLA algorithm is grounded in the concept of memetic evolution, drawing inspiration from a cohort of voracious frogs. This approach amalgamates the attributes of the Particle Swarm Optimization (PSO) algorithm, which relies on social intelligence, with those of the memetic algorithm rooted in genetic evolution. A population of frogs embodies an array of potential solutions, and this assembly of frogs is partitioned into multiple memeplexes, each representing a distinct cultural subset. Recognizing the tendency of frogs to converge around the optimal frog, often a local optimum, specific members within a memeplex are designated as sub-memeplexes to avert premature convergence to local optima. After a specified number of memetic iterations, the memeplexes—constituting the population—are reshuffled. The process of local search and reshuffling is iterated until the desired criterion is met or until the evolutionary generations reach completion (Eusuff et al., 2006; Tosee et al., 2021).

### **Genetic Algorithm (GA)**

Genetic algorithms employ principles drawn from biological, genetic, and evolutionary theories to address complex problems. Each iteration of the algorithm, along with its associated population of potential solutions, is denoted as a generation. Candidate solutions are represented as parameter vectors, with individual components referred to as genes. A population constitutes a collection of these candidate solutions. Throughout the algorithm's execution, a parent candidate solution undergoes modifications to yield a new child (offspring) candidate solution. The core of the evolutionary process involves generating an initial population, assessing their fitness, generating a new set of offspring, and subsequently combining parents and offspring to form a renewed population for the succeeding generation. Termination conditions vary, encompassing factors such as algorithm runtime constraints or the attainment of a predefined target function value. Three genetic operators—namely selection, crossover, and mutation—are harnessed to generate additional individuals or offspring during each generation (Goldberg & Holland, 1988; Katoch et al., 2021; Nikoo et al., 2018). The optimal solution, corresponding to the most favorable fitness value, is denoted as  $x_{\text{BEST}}$ .

## Particle Swarm Optimization (PSO)

Particle swarm optimization (PSO) stands as a robust optimization algorithm, drawing inspiration from the collective behavior observed in bird flocks and fish schools. Within the framework of PSO, a population of particles navigates through the search space in pursuit of the optimal solution. Each particle refines its position and velocity by incorporating insights gleaned from its individual history and the collective experiences of its neighboring particles. PSO exhibits commendable efficacy in tackling an array of optimization challenges encompassing continuous, discrete, single, and multi-objective problems. Its scope extends to addressing issues that exhibit nonlinearity, lack differentiability, or harbor multiple local optima. Nonetheless, it is susceptible to the concern of premature convergence, potentially becoming ensnared within local optima (Eberhart & James Kennedy, 1999; Kennedy & Eberhart, 1995).

## Performance Metrics

Performance metrics are crucial components of regression analysis and machine learning-based prediction models (Plevris et al., 2022). In this work, statistical indicators, such as Average Absolute Error (AAE) and Model Efficiency (EF), are used to evaluate the performance of various topologies. The two metrics are specified as Eq. (1) and Eq. (2) (Li & Heap, 2008), as follows:

$$AAE = \frac{\sum_{i=1}^n \left| \frac{(O_i - P_i)}{O_i} \right|}{n} \quad (1)$$

$$EF = 1 - \frac{\sum_{i=1}^n (P_i - O_i)^2}{\sum_{i=1}^n (\bar{O}_i + O_i)^2} \quad (2)$$

Where  $O_i$  and  $P_i$  are observed and calculated values,  $\bar{O}_i$  is mean of experimental values and  $n$  is the number of observations or samples.

## METHODOLOGY

The methodology entails the development and validation of a finite element model for a log wall. This process aids in the establishment of the necessary dataset for the implementation of multiple informative models based on ANNs.

### Validation of the Finite Element Model

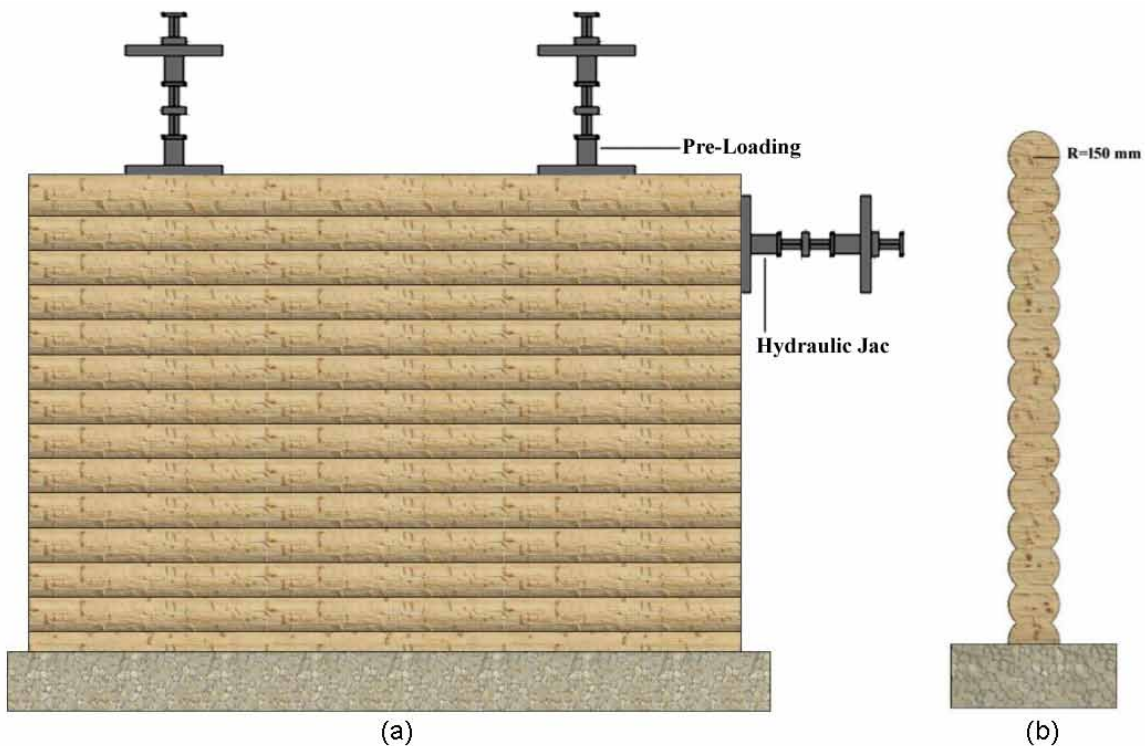
A finite element model of the log wall with a Swedish cope log profile was created in ABAQUS software and verified with the experimental findings published by Fronteik Canada (Popovski, 2002). The FE

## Estimating the In-Plane Lateral Resistance of Reinforced Log Wall Employing Soft Modelling Techniques

model was created for a log wall measuring 2440 mm x 2440 mm, without any corner joinery consisting of eight logs with a diameter of 300 mm, to be consistent with the experimental findings (Popovski, 2002; Popovski et al., 2002). The model employed 3D solid elements of the 8-node, C3D8R type, considering the material properties and boundary conditions aligned with those of the tested wall (Popovski, 2002). Linear elastic behaviour of C24-spruce, classified as an orthotropic material, was assumed for the model. The modulus of elasticity parallel and perpendicular to the grain directions were set to  $E_{0, \text{mean}} = 11,000$  MPa and  $E_{90, \text{mean}} = 370$  MPa, respectively, and the shear modulus of  $G_{\text{mean}} = 690$  MPa was used in the model (Standardization, 2009). The experimental wall setup of the pushover test is reproduced in Figure 2.

In finite element modelling, the interaction mechanism is a crucial aspect in determining the accuracy of the model. The surface-to-surface interactions were defined for the entire length of the logs. The normal behaviour, representing compressive pressure, was set as hard contact preventing penetration between the two surfaces, while the tangential behaviour was determined by the friction coefficient. In this study, a static friction coefficient of 0.65 was used, and the penalty approach was employed defining the tangential behaviour between timber-to-timber interfaces. Since the experimental study was conducted on handcrafted logs, the static friction coefficient of 0.65 was assumed to match the experimental test results. The movement of the sill log, connected to the floor, was restricted in all directions ( $X=0$ ,  $Y=0$  and  $Z=0$ ), while the wall was allowed to move in the longitudinal direction of the logs under lateral loads. The logs stacked horizontally were compressed by vertical loads of 10 kN/m, followed by the application of horizontal displacement. The mesh parameters were selected to improve the computational efficiency of the FE model while maintaining its accuracy in predictions (Bedon, Rinaldin, et al., 2015; Bedon

Figure 2. Experimental set up performed on log-wall



& Fragiaco, 2018). The developed FE model was able to accurately predict the lateral performance of the log wall, as good agreement was seen between the two studies with an average difference of 8%, indicating that the simplified geometry and generalized boundary conditions were effective. Figure 3a illustrates the load-displacement curves produced by the numerical (this study) and experimental studies (Popovski, 2002), and the deformed shape of the wall is displayed in Figure 3b.

### Parametric Analyses

The validated FE model was redesigned, including steel pins of diameter 40 mm. Figure 4 demonstrates the dimension details and the layout of the steel pins in log walls with and without window and door openings. Lastly, an extensive parametric investigation was conducted, resulting in the generation of a dataset comprising log walls featuring crucial variable parameters. This dataset serves as the foundation for devising ANN models based on optimization algorithms. These models are designed to accurately ascertain the maximum in-plane resistance force exhibited by the log wall. The arrangement of diverse input parameters led to the acquisition of 71 distinct samples of log walls. The designated ranges of input parameters employed in the parametric study are detailed in Table 1. Furthermore, Table 2 presents the statistical characteristics of these input parameters. In Figure 5, a depiction of stress distribution in sectional profiles of log walls is presented, comparing the presence of steel rods with and without opening. The figure imparts visual insights into how the addition of steel rods and openings influences the distribution of stress within the log walls.

The distribution of the selected parameters underwent statistical evaluation, with the results presented in Figure 6 using a violin plot. This plot effectively illustrates the distribution of different parametric variations by means of probability density curves. Observing the figure reveals that the vertical axis of the plot corresponds to the density of data points, while the interquartile range (IQR) and median serve as indicators of data dispersion and central tendency. The IQR is reflective of the data's range spanning between the 25<sup>th</sup> and 75<sup>th</sup> percentiles within the distribution.

Figure 3. (a) Experimental and numerical model comparison, (b) stress distribution and model deformation

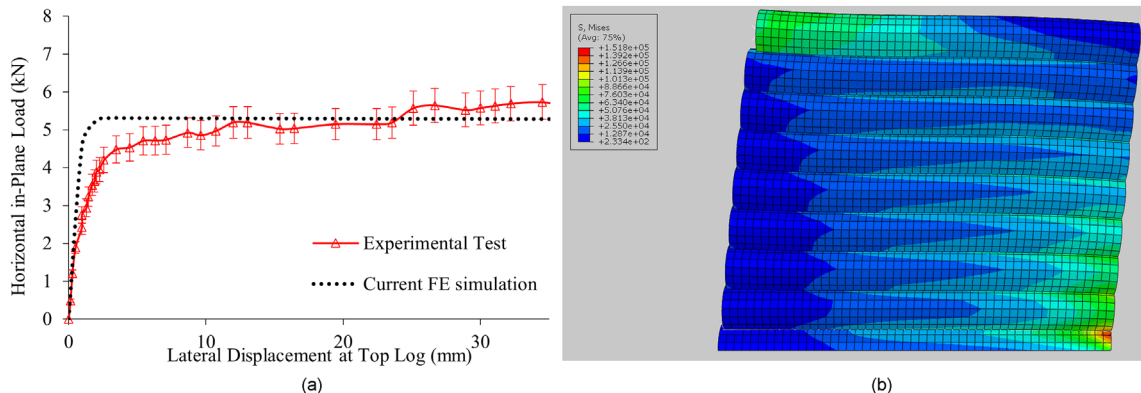


Figure 4. (a) Log wall with window opening, (b) log wall with door opening

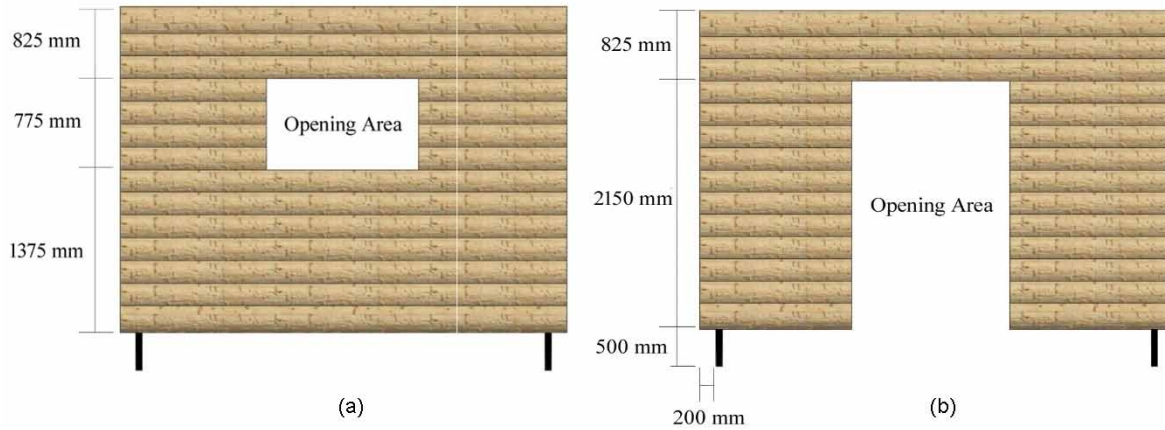


Table 1. Parametric study variants

Num	Parameter	Unit	Values			
1	Friction coefficient	-	0.4	0.5	0.6	-
2	Wall length	m	3	3.5	4	-
3	Window area ( $L \times H$ )	m <sup>2</sup>	1.0×0.75	1.25×0.75	1.50×0.75	-
4	Door area ( $L \times H$ )	m <sup>2</sup>	0.9×2.15	1×2.25	1.1×2.25	1.2×2.25

Table 2. Statistical characteristics of the data used

Parameter	Unit	Type	Minimum	Maximum
Friction Coefficient	-	Input	0.4	0.6
Wall Length	m		3	4
Door Area	m <sup>2</sup>		0	2.58
Window Area	m <sup>2</sup>		0	1.125
Max Force	N	Output	4813.65	11327.8

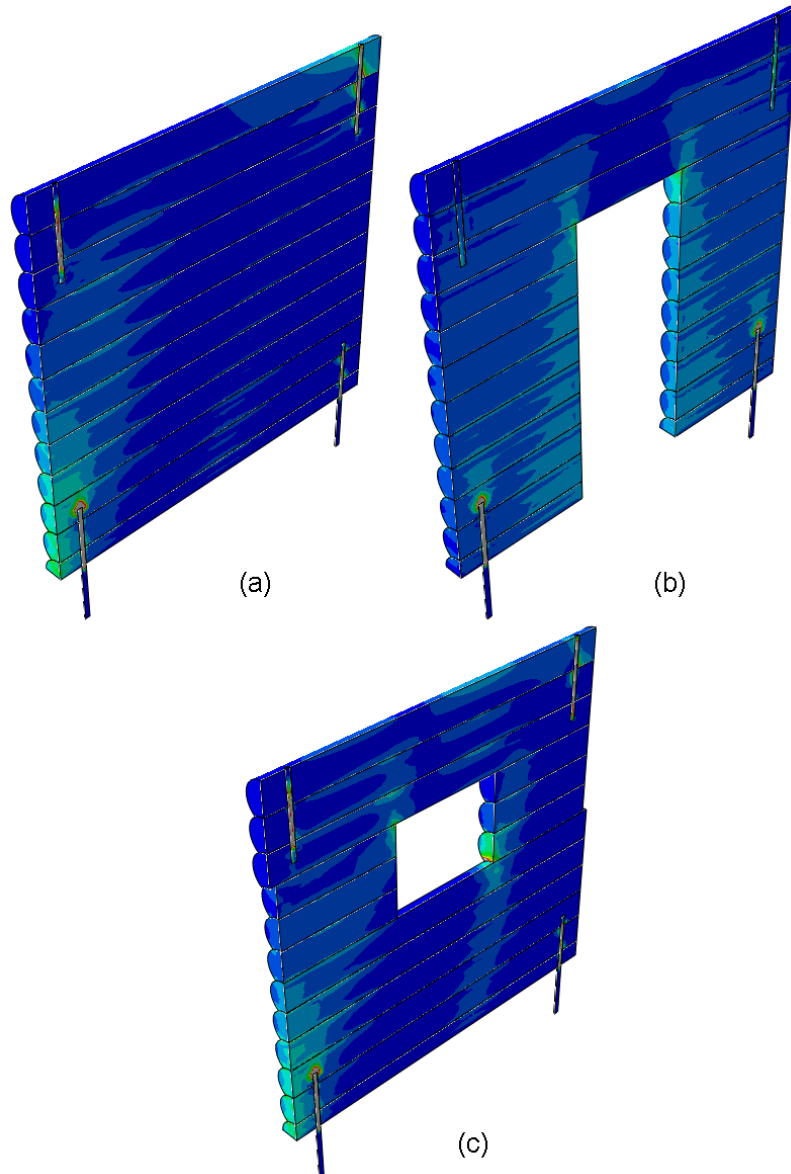
## ANN Model Combined With Shuffled Frog Leaping Algorithm (SFLA)

The neural network utilized in this work is the Feed Forward model. The input variables selected for the estimation of the maximum resistance force encompass the coefficient of friction, the length of the log wall, and the areas of the openings (windows and doors). Given that the neural network models calculate the maximum resistance force utilizing these four input parameters, the trained ANNs are configured with four neurons in the input layer and a single neuron in the output layer.

A total of 71 samples were utilized for estimating the maximum resistance force. Consequently, the dataset underwent a random partitioning into training and testing subsets. Specifically, 70% of the data (57 samples) were allocated to the training set, while the remaining 30% (14 samples) were reserved for

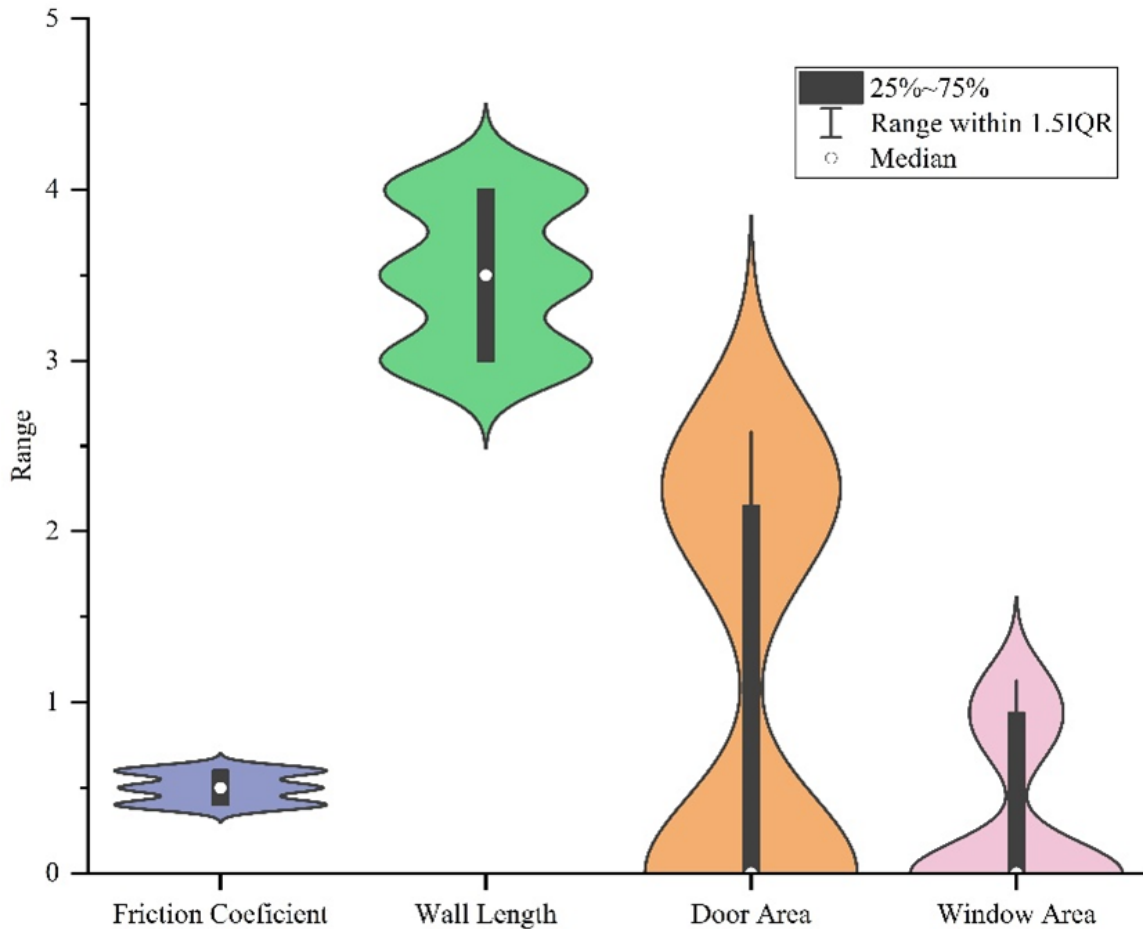
## Estimating the In-Plane Lateral Resistance of Reinforced Log Wall Employing Soft Modelling Techniques

Figure 5. Stress distribution in log walls: cross-sectional view (a) log wall without openings, (b) log wall with door opening, (c) Log WALL with window opening



the testing set. The first hidden layer of the ANN models consists of a range of 1 to 6 neurons, while the second hidden layer encompasses 1 to 5 neurons. This configuration necessitated the training of 30 distinct ANN models. In the case of all ANNs, diverse excitation functions were integrated, encompassing tangent sigmoid (TANSIG), linear (PURELIN), positive linear (POSLIN), and logarithmic sigmoid (LOGSIG) functions, applied to both the hidden and output layers. The neural networks and shuffled frog leaping algorithm (SFLA) were implemented using MATLAB software, with the ANN undergoing training to iteratively adjust the neural network's weights and biases in an effort to minimize the

Figure 6. Violin plots of the input parameters



prediction error. The properties of various ANN topologies are provided in Tables 3 and 4 (Tosee et al., 2021), respectively.

Figure 7 displays the  $R^2$  values corresponding to the training and testing phases across various topologies. Each figure presents the top three models selected from the comprehensive set of 30 neural network models, all of which were optimized using SFLA. The SFLA-ANN 2L(4-4) model has the highest  $R^2$  value indicating the high accuracy of this model compared to similar models.

A total of 30 unique ANN configurations featuring dual hidden layers were constructed and subsequently trained utilizing the shuffled frog-leaping algorithm. The effectiveness of these models was evaluated through the utilization of metrics such as Average Absolute Error (AAE), Efficiency Factor (EF), and coefficient of determination ( $R^2$ ). Within Table 5, the statistical attributes of the three most proficient models are detailed in comparison to other topologies. Figure 8 visually represents the Mean Squared Error (MSE) during the training phase for the foremost three models after the completion of 100 epochs. The findings illustrate that within the same topology, the SFLA-ANN 2L(4-4) configuration boasts the lowest AAE and the highest  $R^2$  values. In Figure 9, the proposed structure of the feed-forward network optimized by the shuffled frog-leaping algorithm is depicted.

*Table 3. Different topologies used in ANNs*

Num	Neurons in Hidden Layer 1	Neurons in Hidden Layer 2	Transfer Functions in Hidden Layers	Transfer Functions in Output Layer	Num	Neurons in Hidden Layer 1	Neurons in Hidden Layer 2	Transfer Functions in Hidden Layers	Transfer Functions in Output Layer
1	1	1	PURELIN	PURELIN	16	4	1	PURELIN	PURELIN
2	1	2	POSLIN	PURELIN	17	4	2	POSLIN	PURELIN
3	1	3	LOGSIG	PURELIN	18	4	3	LOGSIG	PURELIN
4	1	4	TANSIG	PURELIN	19	4	4	TANSIG	PURELIN
5	1	5	TANSIG	TANSIG	20	4	5	TANSIG	TANSIG
6	2	1	PURELIN	PURELIN	21	5	1	PURELIN	PURELIN
7	2	2	POSLIN	PURELIN	22	5	2	POSLIN	PURELIN
8	2	3	LOGSIG	PURELIN	23	5	3	LOGSIG	PURELIN
9	2	4	TANSIG	PURELIN	24	5	4	TANSIG	PURELIN
10	2	5	TANSIG	TANSIG	25	5	5	TANSIG	TANSIG
11	3	1	PURELIN	PURELIN	26	6	1	PURELIN	PURELIN
12	3	2	POSLIN	PURELIN	27	6	2	POSLIN	PURELIN
13	3	3	LOGSIG	PURELIN	28	6	3	LOGSIG	PURELIN
14	3	4	TANSIG	PURELIN	29	6	4	TANSIG	PURELIN
15	3	5	TANSIG	TANSIG	30	6	5	TANSIG	TANSIG

*Table 4. Shuffled frog-leaping algorithm parameters*

Parameter	Value	Parameter	Value
Memplex Size	7	Number of Parents	2
Number of Memplexes	3	Number of Offspring	3
Population Size	Memplex Size * Number of Memplexes	Maximum Number of Iterations	5

To visually demonstrate the performance of the SFLA-ANN 2L (4-4) configuration, Figure 10 portrays the comparison between the estimated and experimental values of the empirical model during both the training and testing phases. The proximity of the model’s estimated values to the reference line ( $y=x$ ) reflects the desirable accuracy achieved by the model.

### **Accuracy of other Informational Models**

Two optimization methodologies, genetic algorithms (GA) and particle swarm optimization (PSO) combined with an ANN, as well as a simple multiple linear regression (MLR) model, were developed and evaluated to validate the SFLA-ANN model presented in this work.

#### **Genetic Algorithm (GA)**

The genetic algorithm was used to train the thirty ANN structures included in Table 3. The properties of the optimal network topology of GA are provided in Table 6 (Tosee et al., 2021). Several topologies were utilized to define the genetic algorithm and the performance of the GA-ANN 2L (4-3) model was

*Figure 7. R<sup>2</sup> values for the proposed topologies in training and testing phases for SFLA-ANN models (a) training set, (b) testing set*

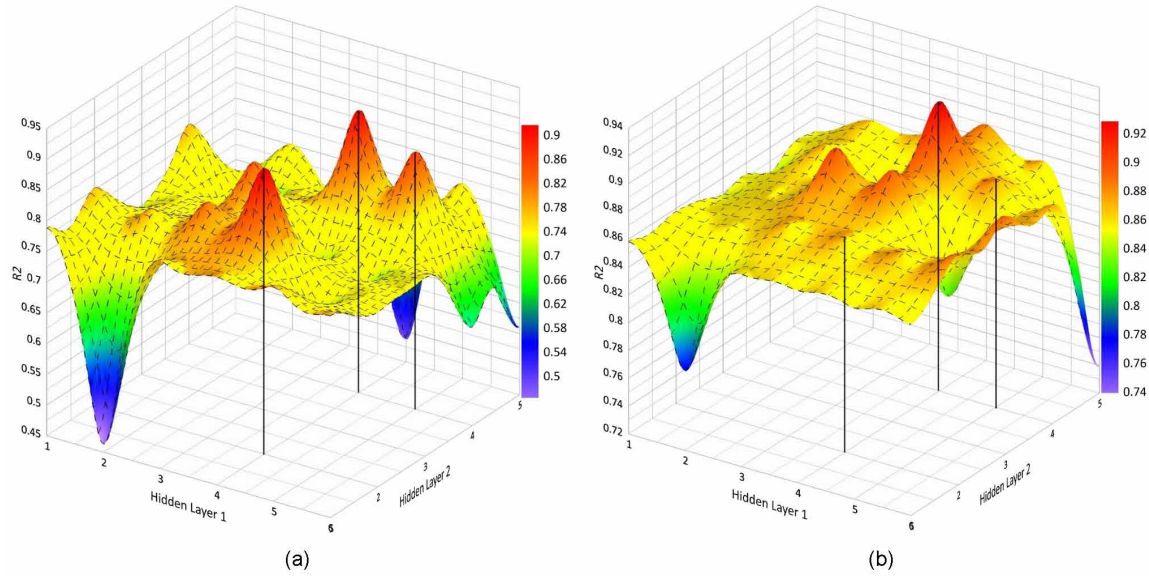


*Table 5. Statistics of the leading two SFLA-ANNs for calculating maximum resistance force*

Model	Training set				Testing set			
	AAE	EF	y=ax+b	R <sup>2</sup>	AAE	EF	y=ax+b	R <sup>2</sup>
SFLA-ANN 2L(4-2)	0.05	0.87	y = 0.8693x + 1099.5	0.87	0.05	0.88	y = 0.75x + 2165.1	0.89
SFLA-ANN 2L(4-4)	0.05	0.91	y = 1.0468x - 367.94	0.93	0.07	0.66	y = 1.3159x - 2209.4	0.91
SFLA-ANN 2L(5-4)	0.04	0.88	y = 0.8933x + 790.74	0.88	0.05	0.87	y = 0.7705x + 1998.7	0.87

found the best among others. In Table 7, the correlation coefficient R<sup>2</sup> for the proposed GA-ANN 2L (4-3) model are 0.89 and 0.88 for the training and the testing phases, respectively.

### Particle Swarm Optimization (PSO)

The present study utilized the particle swarm optimization (PSO) algorithm for training thirty different artificial neural network (ANN) structures, as listed in Table 3. The properties of the optimal network topology obtained via the PSO algorithm are provided in Table 8 (Sadowski et al., 2019). Various network topologies were evaluated, and the PSO-ANN 2L (3-3) model demonstrated superior performance compared to other configurations. The proposed PSO-ANN 2L (3-3) model achieved a high correlation coefficient (R<sup>2</sup>) of 0.87 for both the training and testing phases, as presented in Table 9.

*Figure 8. MSE train for top three models SFLA-ANN*

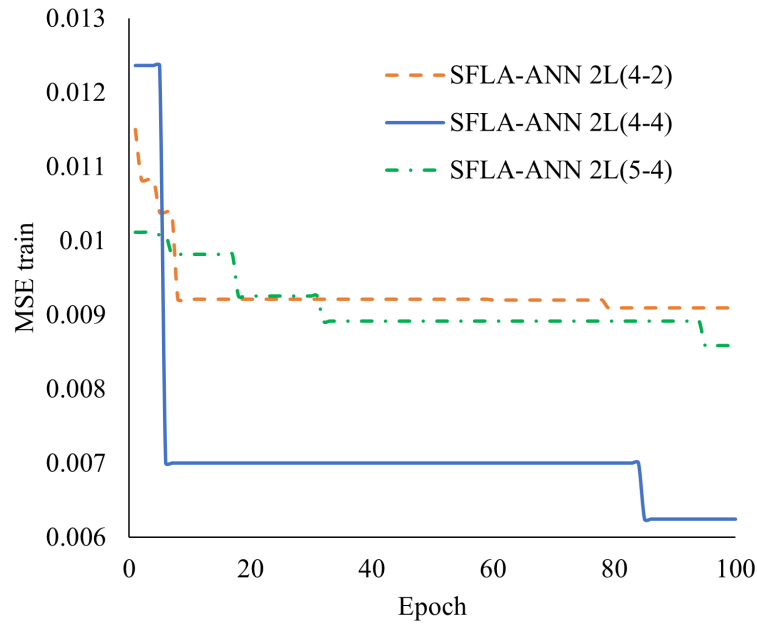
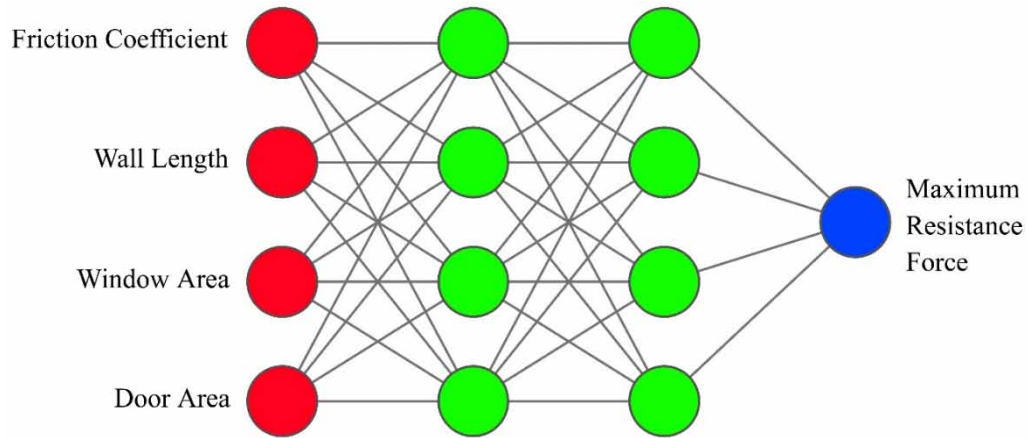


*Figure 9. The architecture of the 4-4-4-1 topology ANN used in this study*



### Multiple Linear Regression (MLR)

The linear regression technique posits the presence of a linear association between two variables in order to ascertain their fundamental connection. Multiple linear regression (MLR) falls within the realm of linear regression, operating on the basis of multiple input variables (Khademi; et al., 2017). Within regression analysis, the variables - whether input or output - can either be independent or dependent on one another. In the context of this study, numerous MLR models were formulated and evaluated concerning input variables and the parameters related to maximum resistance force. The coefficients

## Estimating the In-Plane Lateral Resistance of Reinforced Log Wall Employing Soft Modelling Techniques

Figure 10. Observation and computed values for maximum resistance force using (a) training data and (b) testing data for the SFLA-ANN 2L(4-4) model

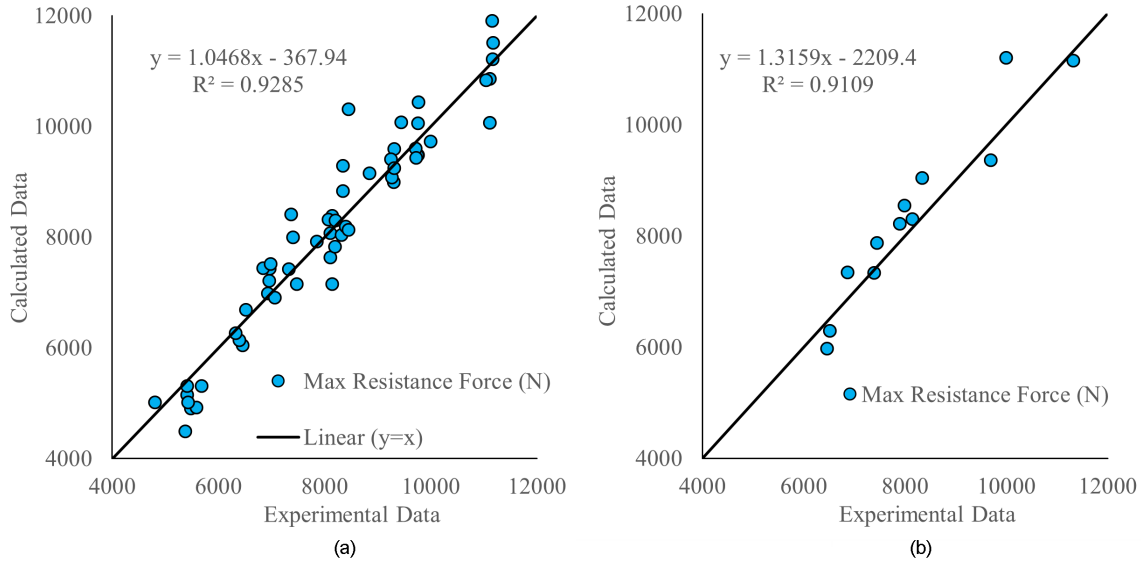


Table 6. Characteristics of the genetic algorithm

Parameter	Value
Max generations	100
Recombination (%)	15
Lower/Upper bound	[-1, 1]
Crossover (%)	50
Crossover method	Single point
Selection mode	1
Population size	150

Table 7. Statistics of the top three GA-ANNs for determining maximum resistance force

Model	Train				Test			
	AAE	EF	$y=ax+b$	$R^2$	AAE	EF	$y=ax+b$	$R^2$
GA-ANN 2L(4-2)	0.06	0.83	$y = 0.8805x + 1042.4$	0.84	0.06	0.82	$y = 0.8018x + 1863.4$	0.82
GA-ANN 2L(4-3)	0.04	0.88	$y = 0.9276x + 653.01$	0.89	0.05	0.86	$y = 0.907x + 1056.3$	0.88
GA-ANN 2L(3-3)	0.06	0.86	$y = 0.8664x + 1193.4$	0.86	0.06	0.88	$y = 0.8583x + 1252.6$	0.88

outlined in Eq. (3) have been optimized to effectively determine the maximum resistance force through employment of the MLR model.

$$y = -7350 + 13946 \times x_1 + 2672 \times x_2 - 318 \times x_3 - 913 \times x_4 \quad (3)$$

*Table 8. Characteristics of the particle swarm optimization*

Parameter	Value
Swarm size	100
Cognition coefficient	2
Social coefficient	2
Generation	100

*Table 9. Statistics of the top three PSO-ANNs for determining maximum resistance force*

Model	Train				Test			
	AAE	EF	$y=ax+b$	$R^2$	AAE	EF	$y=ax+b$	$R^2$
PSO-ANN 2L(3-3)	0.05	0.86	$y = 0.8548x + 1260.4$	0.87	0.05	0.88	$y = 0.8643x + 1203.6$	0.87
PSO-ANN 2L(6-2)	0.06	0.83	$y = 0.8805x + 1042.4$	0.84	0.06	0.82	$y = 0.8018x + 1863.4$	0.82
PSO-ANN 2L(5-3)	0.05	0.87	$y = 0.8652x + 1191.4$	0.87	0.06	0.85	$y = 0.7464x + 2277.5$	0.86

Where  $y$  is the maximum resistance force,  $x_1$  is the friction coefficient,  $x_2$  is the wall length and  $x_3$  and  $x_4$  are door area and window area, respectively. As shown in Table 10, the correlation coefficient,  $R^2$ , for the proposed MLR model is 0.86 for the training phase and 0.81 for the testing phase.

### Comparison of the Accuracy of the Models

The estimation of the maximum resistance force was achieved through the implementation of several informative and analytical models, namely SFLA-ANN, GA-ANN, PSO-ANN, and MLR. These models were constructed leveraging the dimensional and physical attributes of the log wall. As depicted in Table 11, the comparison is based on statistical metrics encompassing the minimal error, namely AAE, EF, slope of the linear fit, and  $R^2$ . The findings conclusively illustrate that the SFLA-ANN 2L(4-4) model outperforms the other models significantly. This is evidenced by its superior flexibility and accuracy, as denoted by its highest EF,  $R^2$ , and linear fit slope values, as well as its lowest AAE values.

Figure 11 illustrates the predictions generated by each individual model. The outcomes reveal that an ANN optimized with the SFLA is capable of precisely forecasting the maximum resistance force exhibited by log walls.

In Figure 12, a Taylor diagram showcases metrics such as root-mean-square difference (RMSD), correlation coefficient, and standard deviation for the SFLA-ANN, GA-ANN, PSO-ANN, and MLR models. The results highlight the superior accuracy and adaptability of the SFLA-ANN model, optimized using the shuffled frog leaping algorithm, compared to the other models.

*Table 10. Statistics of MLR models for determining maximum resistance force*

Model	Train				Test			
	AAE	EF	$y=ax+b$	$R^2$	AAE	EF	$y=ax+b$	$R^2$
MLR	0.05	0.86	$y = 0.8664x + 1095.7$	0.86	0.05	0.81	$y = 0.76x + 2067.9$	0.81

## Estimating the In-Plane Lateral Resistance of Reinforced Log Wall Employing Soft Modelling Techniques

Table 11. Statistics of different models for determining maximum resistance force

Model	All Dataset			
	AAE	EF	$y=ax+b$	$R^2$
SFLA-ANN 2L(4-4)	0.06	0.86	$y = 1.1065x - 768.48$	0.91
MLR	0.05	0.85	$y = 0.8481x + 1258.4$	0.85
GA-ANN 2L(4-3)	0.04	0.88	$y = 0.9287x + 688.34$	0.88
PSO-ANN 2L(3-3)	0.05	0.87	$y = 0.8571x + 1246.4$	0.87

Figure 11. Maximum resistance force observation and calculated values for different models utilizing the complete dataset (a) SFLA-ANN (b) MLR (c) GA-ANN (d) PSO-ANN

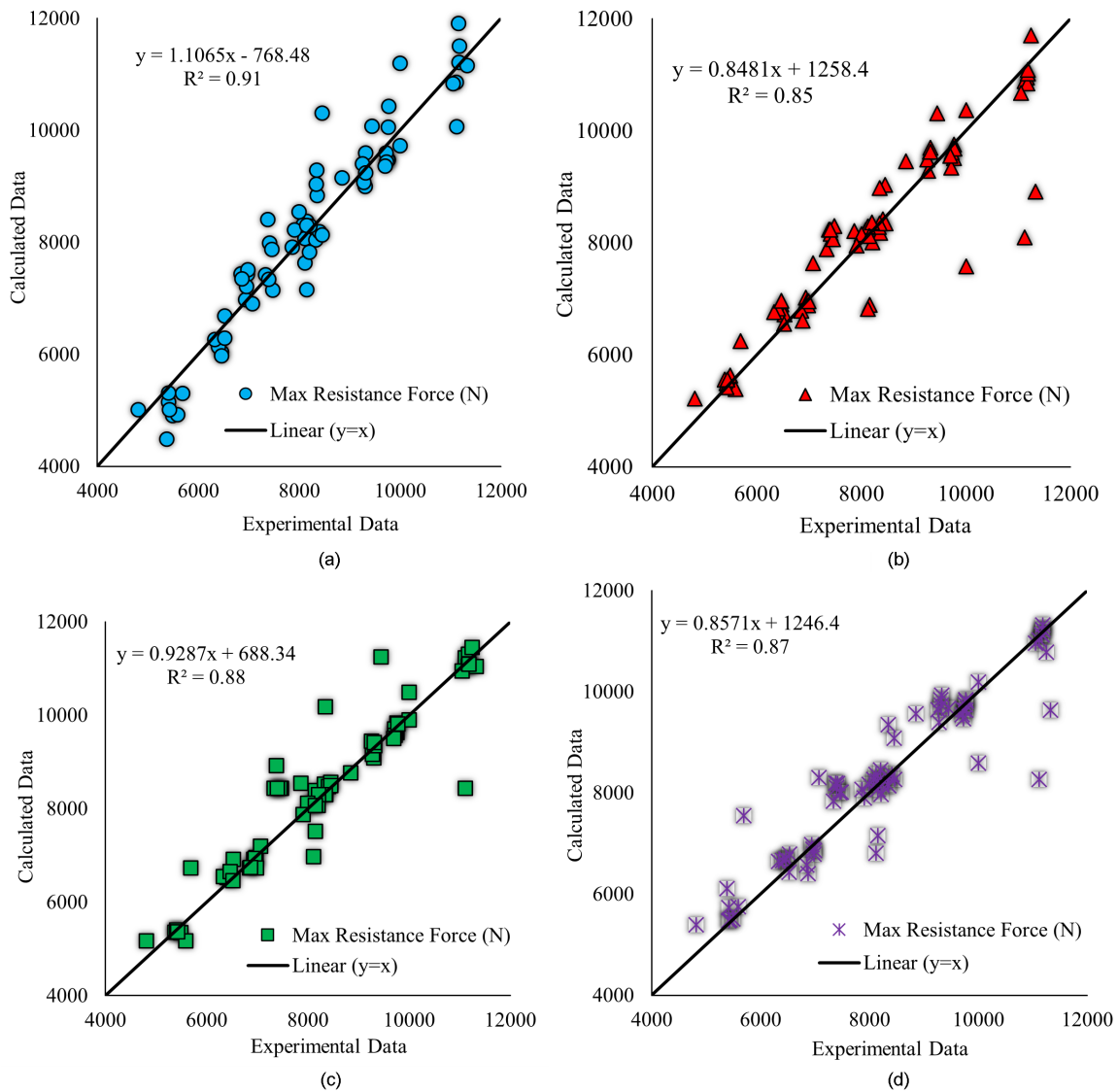
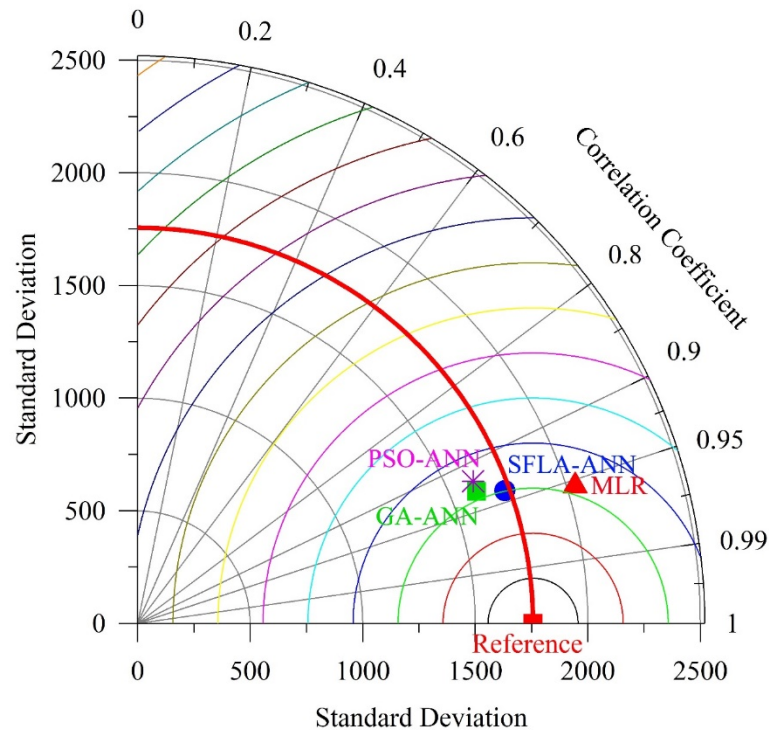


Figure 12. Taylor diagram visualization of model performance in terms of Maximum force



## CONCLUSION

This study aimed to evaluate various models, employing SFLA, GA, PSO, and MLR approaches, for predicting the maximum resistance force in log walls. Among these models, the SFLA-ANN 2L (4-4), integrating the Shuffled Frog Leaping Algorithm (SFLA) with artificial neural networks (ANN), demonstrated the highest accuracy. Additionally, the study found that the GA-ANN 2L (4-3) model outperformed those developed using PSO, following the topology 2L (3-3).

Furthermore, multiple linear regression (MLR) techniques were utilized to formulate another set of models. These models showed relatively lower accuracy compared to the others. The study's findings emphasize the proficiency of the SFLA-based ANN model in accurately estimating the lateral resistance of log walls. This proposed model holds promise in aiding engineers to rapidly and precisely assess the lateral capacity of log walls, thereby streamlining the process without compromising accuracy.

## FUTURE STUDIES

The authors intend to carry out experimental investigations on log walls with different log profiles to corroborate the numerical findings using the dataset generated at Concordia University. In forthcoming studies, sophisticated algorithms such as the Gray Wolf Optimizer (Mirjalili et al., 2014), Whale Optimization Algorithm (Mirjalili & Lewis, 2016), and Bat Algorithm (Aalimahmoodi et al., 2021; Yang, 2010) will be employed to evaluate the in-plane lateral resistance of reinforced log walls.

## CREDIT AUTHOR STATEMENT

**K.G.M. Kandethanthri:** Formal Analysis, Data Collection, Validation, Finite Element Models. **Mehdi Nikoo:** Conceptualization, Methodology, Investigation, Writing- Original Draft Preparation, Review and Editing. **Ghazanfarah Hafeez:** Supervision, Conceptualization, Methodology, Investigation, Writing, Review and Editing, **Ashutosh Bagchi:** Methodology, Investigation, Visualization, Review and Editing, **Vagelis Plevris:** Methodology, Investigation, Visualization, Review and Editing,

## DATA AVAILABILITY STATEMENT

Some or all data, models, or code that support the findings of this study are available from the corresponding author upon reasonable request.

## REFERENCES

- Aalimahmoody, N., Bedon, C., Hasanzadeh-Inanlou, N., Hasanzade-Inallu, A., & Nikoo, M. (2021). BAT Algorithm-Based ANN to Predict the Compressive Strength of Concrete—A Comparative Study. *Infrastructures*, 6(6), 80. doi:10.3390/infrastructures6060080
- Adeli, H. (2001). Neural Networks in Civil Engineering: 1989–2000. *Computer-Aided Civil and Infrastructure Engineering*, 16(2), 126–142. doi:10.1111/0885-9507.00219
- Bardak, S., Tiryaki, S., Nemli, G., & Aydın, A. (2016). Investigation and neural network prediction of wood bonding quality based on pressing conditions. *International Journal of Adhesion and Adhesives*, 68, 115–123. doi:10.1016/j.ijadhadh.2016.02.010
- Bedon, C., & Fragiacomio, M. (2017). Derivation of buckling design curves via FE modelling for in-plane compressed timber log-walls in accordance with the Eurocode 5. *Holz als Roh- und Werkstoff*, 75(3), 449–465. doi:10.1007/s00107-016-1083-5
- Bedon, C., & Fragiacomio, M. (2018). Numerical Investigation of Timber Log-Haus Walls with Steel Dovetail Reinforcements under In-Plane Seismic Loads. *Advances in Civil Engineering*, 6929856, 1–12. Advance online publication. doi:10.1155/2018/6929856
- Bedon, C., & Fragiacomio, M. (2019). Experimental and numerical analysis of in-plane compressed unprotected log-haus timber walls in fire conditions. *Fire Safety Journal*, 107, 89–103. doi:10.1016/j.firesaf.2017.12.007
- Bedon, C., Massimo, F., Claudio, A., & Carlotta, S. (2015). Experimental Study and Numerical Investigation of Blockhaus Shear Walls Subjected to In-Plane Seismic Loads. *Journal of Structural Engineering*, 141(4), 4014118. doi:10.1061/(ASCE)ST.1943-541X.0001065
- Bedon, C., Rinaldin, G., & Fragiacomio, M. (2015). Non-linear modelling of the in-plane seismic behaviour of timber Blockhaus log-walls. *Engineering Structures*, 91, 112–124. doi:10.1016/j.engstruct.2015.03.002

## ***Estimating the In-Plane Lateral Resistance of Reinforced Log Wall Employing Soft Modelling Techniques***

- Bishop, C. (2006). *Pattern Recognition and Machine Learning*. Springer-Verlag. <https://www.springer.com/gp/book/9780387310732>
- Branco, J. M., & Araújo, J. P. (2012). Structural behaviour of log timber walls under lateral in-plane loads. *Engineering Structures*, *40*, 371–382. doi:10.1016/j.engstruct.2012.03.004
- Branco, J. M., & Araújo, J. P. C. (2010). *Lateral resistance of log timber walls subjected to horizontal loads*. Academic Press.
- De Araujo, V., Barbosa, J., Garcia, J., Gava, M., Laroca, C., & César, S. (2016). Woodframe: Light Framing Houses for Developing Countries. *Revista de la Construcción*, *15*(2), 78–87. doi:10.4067/S0718-915X2016000200008
- Eakintumas, W., Pulngern, T., Rosarpitak, V., & Sombatsompop, N. (2022). Finite Element Modeling and Experimental Investigation for Wood/PVC Composites Log-Walls under In-Plane Lateral Load. *Polymers*, *14*(21), 4673. Advance online publication. doi:10.3390/polym14214673 PMID:36365666
- Eberhart, R., & Kennedy, J. (1999). A New Optimizer Using Particle Swarm Theory. *International Symposium on Micro Machine and Human Science*.
- Eusuff, M., Lansey, K., & Pasha, F. (2006). Shuffled frog-leaping algorithm: A memetic meta-heuristic for discrete optimization. *Engineering Optimization*, *38*(2), 129–154. doi:10.1080/03052150500384759
- Goldberg, D. E., & Holland, J. H. (1988). Genetic Algorithms and Machine Learning. *Machine Learning*, *3*(2), 95–99. doi:10.1023/A:1022602019183
- Graham Drew, A., Carradine David, M., Bender Donald, A., & Daniel, D. J. (2010). Performance of Log Shear Walls Subjected to Monotonic and Reverse-Cyclic Loading. *Journal of Structural Engineering*, *136*(1), 37–45. doi:10.1061/(ASCE)ST.1943-541X.0000035
- Grossi, P., Sartori, T., Giongo, I., & Tomasi, R. (2016). Analysis of timber log-house construction system via experimental testing and analytical modelling. *Construction & Building Materials*, *102*, 1127–1144. doi:10.1016/j.conbuildmat.2015.10.067
- Hahney, T. (2000). *How Log Buildings Resist Lateral Loads*. Academic Press.
- Haykin, S. (2008). *Neural Networks and Learning Machines*. Pearson.
- Heimeshoff, B., & Kneidl, R. (1990). Abtragung vertikaler Lasten in Blockwänden. IRB-Verlag.
- Heimeshoff, B., & Kneidl, R. (1992). Bemessungsverfahren zur Abtragung vertikaler Lasten in Blockwänden. Holz Als Roh-Und Werkstoff. doi:10.1007/BF02662783
- Ian, F., & Nabil, K. (1994). Neural Networks in Civil Engineering. I: Principles and Understanding. *Journal of Computing in Civil Engineering*, *8*(2), 131–148. doi:10.1061/(ASCE)0887-3801(1994)8:2(131)
- Kalantari, R., Abbasi Malekabadi, R., & Hafeez, G. (2021). *Lateral Performance of Log Wall with Butt-And-Pass Corner Style*. Canadian Society for Civil Engineering. CSCE.

## ***Estimating the In-Plane Lateral Resistance of Reinforced Log Wall Employing Soft Modelling Techniques***

Kalantari, R., & Hafeez, G. (2021). Finite Element Modelling of Log Wall Corner Joints. *World Academy of Science, Engineering and Technology. International Journal of Structural and Construction Engineering*, 15(12), 472–477.

Kandethanthri, K. G. M., & Hafeez, G. (2023). Investigating the structural response of log walls to lateral loading: A parametric study of geometric and material parameters. *Mechanics of Advanced Materials and Structures*, 1–12. doi:10.1080/15376494.2023.2212649

Katoch, S., Chauhan, S. S., & Kumar, V. (2021). A review on genetic algorithm: Past, present, and future. *Multimedia Tools and Applications*, 80(5), 8091–8126. doi:10.1007/s11042-020-10139-6 PMID:33162782

Kennedy, J., & Eberhart, R. (1995). Particle swarm optimization. *Proceedings of ICNN'95 - International Conference on Neural Networks*, 4, 1942–194. 10.1109/ICNN.1995.488968

Khademi, F., Akbari, M., Jamal, S. M., & Nikoo, M. (2017). Multiple linear regression, artificial neural network, and fuzzy logic prediction of 28 days compressive strength of concrete. *Frontiers of Structural and Civil Engineering*, 11(1), 90–99. doi:10.1007/s11709-016-0363-9

Li, J., & Heap, A. D. (2008). *A Review of Spatial Interpolation Methods for Environmental Scientists*. Geoscience Australia.

Ma, W., Wang, W., & Cao, Y. (2022). Mechanical Properties of Wood Prediction Based on the NAGGWO-BP Neural Network. In *Forests* (Vol. 13, Issue 11). doi:10.3390/f13111870

Mirjalili, S., & Lewis, A. (2016). The Whale Optimization Algorithm. *Advances in Engineering Software*, 95(Supplement C), 51–67. doi:10.1016/j.advengsoft.2016.01.008

Mirjalili, S., Mirjalili, S. M., & Lewis, A. (2014). Grey Wolf Optimizer. *Advances in Engineering Software*, 69(Supplement C), 46–61. doi:10.1016/j.advengsoft.2013.12.007

Nikoo, M., Hadzima-Nyarko, M., Nyarko, E. K., & Nikoo, M. (2018). Determining the Natural Frequency of Cantilever Beams Using ANN and Heuristic Search. *Applied Artificial Intelligence*, 32(3), 309–334. doi:10.1080/08839514.2018.1448003

Nikoo, M., Hafeez, G., Doudak, G., & Plevris, V. (2023). Predicting the Fundamental Period of Light-Frame Wooden Buildings by Employing Bat Algorithm-Based Artificial Neural Network. In *Artificial Intelligence and Machine Learning Techniques for Civil Engineering* (pp. 139–162). IGI Global. doi:10.4018/978-1-6684-5643-9.ch006

Plevris, V., Solorzano, G., Bakas, N. P., & Ben Seghier, M. E. A. (2022). Investigation of performance metrics in regression analysis and machine learning-based prediction models. *8th European Congress on Computational Methods in Applied Sciences and Engineering (ECCOMAS Congress 2022)*. 10.23967/eccomas.2022.155

Popovski, M. (2002). *Testing of lateral resistance of handcrafted log walls Phase I and II*. Academic Press.

Popovski, M., Deacon, B., & Karacabeyli, E. (2002). Testing of lateral resistance of handcrafted log walls Phase I and II. International Log Builders Association.

### ***Estimating the In-Plane Lateral Resistance of Reinforced Log Wall Employing Soft Modelling Techniques***

Rinaldin, G., Poh'si , G., Amadio, C., & Fragiacom, M. (2013). Modelling of seismic behaviour of light-frame timber structures. *Ingenier a S smica*, 30, 82–98.

Sadowski,  ., Nikoo, M., Shariq, M., Joker, E., & Czarnecki, S. (2019). The Nature-Inspired Metaheuristic Method for Predicting the Creep Strain of Green Concrete Containing Ground Granulated Blast Furnace Slag. *Materials (Basel)*, 12(2), 293. Advance online publication. doi:10.3390/ma12020293 PMID:30658508

Sciomenta, M., Bedon, C., Fragiacom, M., & Luongo, A. (2018). Shear Performance Assessment of Timber Log-House Walls under In-Plane Lateral Loads via Numerical and Analytical Modelling. In *Buildings* (Vol. 8, Issue 8). MDPI. doi:10.3390/buildings8080099

Scott, R. J., Leichti, R., & Miller, T. H. (2005). An experimental investigation of foundation anchorage details and base shear capacity for log buildings. *Forest Products Journal*, 55, 38–45.

Standardization, E. C. (2009). *Structural timber-strength classes-EN 338*. Academic Press.

Tiryaki, S., & Aydın, A. (2014). An artificial neural network model for predicting compression strength of heat treated woods and comparison with a multiple linear regression model. *Construction & Building Materials*, 62, 102–108. doi:10.1016/j.conbuildmat.2014.03.041

Tosee, S. V., Faridmehr, I., Bedon, C., Sadowski,  ., Aalimahmoody, N., Nikoo, M., & Nowobilski, T. (2021). Metaheuristic Prediction of the Compressive Strength of Environmentally Friendly Concrete Modified with Eggshell Powder Using the Hybrid ANN-SFL Optimization Algorithm. *Materials (Basel)*, 14(20), 6172. Advance online publication. doi:10.3390/ma14206172 PMID:34683782

Yang, X. S. (2010). A new metaheuristic Bat-inspired Algorithm. *Studies in Computational Intelligence*. doi:10.1007/978-3-642-12538-6\_6